Biochemical and Biophysical Research Communications 435 (2013) 702–707

Contents lists available at SciVerse ScienceDirect

Biochemical and Biophysical Research Communications

journal homepage: www.elsevier.com/locate/ybbrc

Sequential signaling cascade of IL-6 and PGC-1α is involved in high glucose-induced podocyte loss and growth arrest

Dong Il Kim, Soo Hyun Park *

College of Veterinary Medicine, Chonnam National University, Gwangju 500 757, Republic of Korea

ARTICLE INFO

Article history:
Received 7 May 2013
Available online 18 May 2013

Keywords:
Diabetic nephropathy
Interleukin 6
PGC-1α
Podocyte loss
Cell arrest

ABSTRACT

Podocyte loss, which is mediated by podocyte apoptosis, is implicated in the onset of diabetic nephropathy. In this study, we investigated the involvement of interleukin (IL)-6 in high glucose-induced apoptosis of rat podocytes. We also examined the pathophysiological role of peroxisome proliferator-activated receptor gamma coactivator-1 alpha (PGC-1α) in this system. High glucose treatment induced not only podocyte apoptosis but also podocyte growth arrest. High glucose treatment also increased IL-6 secretion and activated IL-6 signaling. The high glucose-induced podocyte apoptosis was blocked by IL-6 neutralizing antibody. IL-6 treatment or overexpression induced podocyte apoptosis and growth arrest, and IL-6 siRNA transfection blocked high glucose-induced podocyte apoptosis and growth arrest. Furthermore, high glucose or IL-6 treatment increased PGC-1α expression, and PGC-1α overexpression also induced podocyte apoptosis and growth arrest. PGC-1α siRNA transfection blocked high glucose-induced podocyte apoptosis and growth arrest. Collectively, these findings showed that high glucose promoted apoptosis and cell growth arrest in podocytes *via* IL-6 signaling. In addition, PGC-1α is involved in podocyte apoptosis and cell growth arrest. Therefore, blocking IL-6 and its downstream mediators such as IL6Rα, gp130 and PGC-1α may attenuate the progression of diabetic nephropathy.

1. Introduction

Diabetic nephropathy is one of the most serious complications of both type 1 and type 2 diabetes mellitus, with high mortality. Among the three intrinsic cells in the glomerulus, the podocyte is a pivotal component of the filtration barrier, which has specific cytobiological properties and physiological functions. Podocyte loss, which is mediated by podocyte apoptosis, is implicated in the onset of various kidney diseases, including diabetic nephropathy [1]. Podocyte hypertrophy is a major characteristic of diabetic nephropathy [2], and podocyte loss is preceded by glomerular hypertrophy [3]. Glomerular hypertrophy caused by hyperglycemia is associated with the alteration of p21Cip or p27Kip expression, which induces cell cycle arrest [4].

Interleukin (IL)-6 protein consists of 184 amino acids and is produced by lymphoid cells and a variety of non-lymphoid cells, including podocytes [5]. The synthesis and release of IL-6 are influenced by various pathological conditions. IL-6 acts on its target cells *via* a specific receptor α-subunit, followed by the activation of the common receptor subunit, gp130 [6]. However, the involvement of IL-6 in diabetic nephropathy remains unclear.

Peroxisome proliferator-activated receptor gamma coactivator-1 alpha (PGC-1α), a transcriptional coactivator that plays a role in mitochondrial biogenesis and energy metabolism, is predominantly expressed in the kidney [7]. PGC-1α can interact with diverse nuclear receptors as well as many other transcription factors [8]. Under pathophysiological conditions, the PGC-1α level is increased [9]. However, Benton et al. (2010) reported that PGC-1α improved insulin signaling in the skeletal muscle of insulin-resistant obese Zucker rats [10]. To date, the direct effect of PGC-1α in diabetic nephropathy remains to be determined. Based upon these reports, we hypothesized that signaling molecules such as IL-6 and PGC-1α are associated with high glucose-induced apoptosis of podocytes. Therefore, in the present study, we aimed to elucidate the involvement of IL-6 and PGC-1α in high glucose-induced apoptosis of rat podocytes.

2. Materials and methods

2.1. Materials

Dulbecco's Modified Eagle's Medium (DMEM), Ham's nutrient mixture F-12 and fetal bovine serum (FBS) were purchased from Life Technologies (Gibco BRL, Grand Island, NY, USA). D-glucose,

* Corresponding author. Address: Department of Veterinary Physiology, College of Veterinary Medicine, Chonnam National University, Kwangju 500 757, Republic of Korea. Fax: +82 62 530 2809.
E-mail address: parksh@chonnam.ac.kr (S.H. Park).

0006-291X/$ - see front matter Crown Copyright © 2013 Published by Elsevier Inc. All rights reserved.
http://dx.doi.org/10.1016/j.bbrc.2013.05.046

3-(4,5-dimethylthiazol-2-yl)2,5-diphenyl tetrazolium bromide (MTT), recombinant rat IL-6 and anti-Goat TRITC conjugated secondary antibody were obtained from Sigma–Aldrich (St. Louis, MO, USA). β-Actin antibody, IL-6 antibody, p21Cip antibody, p27Kip antibody, Bcl-2 antibody, gp130 antibody, IL6Rα antibody, anti-Goat HRP conjugated secondary antibody and goat-IgG were purchased from Santa Cruz Biotechnology (Santa Cruz, CA, USA). p53 antibody, Caspase-9 antibody, Caspase-3 antibody and anti-Rabbit HRP conjugated secondary antibody were purchased from Cell Signaling Technology (Beverly, MA, USA). The PGC-1α rabbit polyclonal antibody against a chemically synthesized peptide derived from the region of rat PGC-1α was made by us. All reagents were of the highest purity commercially available.

2.2. Cell cultures

Rat visceral GECs were isolated and characterized as described by Kreisberg et al. [11] These cells were used between passages 10 and 12. The culture medium for glomerular epithelial cells was DMEM/Ham's F-12 (1:1) supplemented with 10% FBS. Glomerular epithelial cells were grown to confluence in 60 mm dishes in DMEM/Ham's F-12 (DMEM, Gibco; F-12 Nutrient Mixture, Gibco; obtained without glucose and then supplemented by adding glucose to the appropriate concentrations) with 15 mM HEPES buffer, 10% FBS, 5.5 mM glucose, 0.35% additional sodium bicarbonate, 2.5 mM L-glutamine and 1% penicillin/streptomycin at 37 °C. The media were changed every other day. Passaged cells were plated to yield near-confluent cultures at the end of the experiments.

2.3. TCA precipitation

TCA stock was added to 4 volume of culture medium that final mixture is 20% TCA. Mixtures were mixed well by vortex and incubated for 30 min on ice. Then the mixtures were centrifuged at 15,000 rpm for 10 min at 4 °C. The supernatants were carefully removed. Leaving pellets were washed with cold acetone then centrifuged at 15,000 rpm for 10 min at 4 °C. Pellets were dried in the room temperature hood. Dried pellets were dissolved with SDS–PAGE sample buffer.

2.4. RNA isolation and RT-qPCR

Total RNA was extracted from the cells using TRIzol, which is a monophasic solution of phenol and guanidine isothiocyanate purchased from (Invitrogen, Carlsbad, CA, USA). Reverse transcription was carried out with 1 μg RNA using an RT Premix reverse transcription system kit (AccuPower, Seoul, Korea) with oligo-dT18 primers. 0.5 Microliter of the RT products was amplified with a Power SYBR Green (Applied Biosystems, Warrington, UK). The primers used were 5′-TTGCCTTCTTGGGACTGATG-3′ (sense), 5′-GCCATTGCACAACTCTTTTC-3′ (antisense) for rat IL-6 and 5′-AGGCCCAGAGCAAGAGAG-3′ (sense), 5′-TCAACATGATCTGGGTCATC-3′ (antisense) for rat β-actin. β-Actin was used as a control to confirm the quantity of the RNA. The RT-qPCR products were analyzed the values of the high glucose treatment group relative to the control group, and standardizing the data relative to β-actin.

2.5. Whole cell preparation and western blotting

The medium was then removed and the cells were washed twice with ice-cold phosphate buffered saline (PBS), scraped and then harvested by microcentrifugation (13,000 rpm for 10 min) and removed supernatant. Pellet was resuspended in M-PER Mammalian Protein Extraction Reagent (Thermo, IL, USA) containing protease inhibitor cocktail (Sigma, Missouri, USA) and phosphatase inhibitor cocktail I + II. (Sigma, Missouri, USA) The resuspended cells were lysed mechanically on ice by vortex. The protein level was quantified using the Bradford procedure. The whole cell (30 μg of protein) were separated by SDS–polyacrylamide gel electrophoresis and transferred to an enhanced nitrocellulose membrane. The blots were then washed with TBST (10 mM Tris–HCl, pH 7.6, 150 mM NaCl, 0.05% Tween-20), blocked with 5% skim milk powder in TBST for 1 h and incubated for 15 h at 4 °C with the primary antibody at the dilutions recommended by the supplier. The membrane was then washed with TBST, and the secondary antibodies conjugated to horseradish peroxidase were incubated for 1 h at room temperature. The bands were visualized using Amersham ECL™ Western Blotting Detection Reagents (GE Healthcare, UK) on X-ray film (Kodak BioMax Light Film).

2.6. Immunofluorescence staining

Podocytes were fixed with 0.5% paraformaldehyde in phosphate-buffered saline (PBS), permeabilized for 10 min with 0.1% (v/v) Triton X-100, and washed three times for 10 min each with PBS. Cells were incubated for 1 h with polyclonal anti-IL-6 primary antibody (1:500) in a solution containing 1% (v/v) BSA in PBS and washed three times for 10 min each with PBS. Cells were incubated with 1% (v/v) BSA for 5 min, incubated for 1 h with TRITC-conjugated secondary antibody in PBS containing 1% (v/v) BSA, and washed three times for 10 min each with PBS. Samples were mounted on slides and visualized with a confocal microscope (Fluoview 300; Olympus, Tokyo; http://www.olympusglobal.com).

2.7. MTT assay

Cells were set up (2×10^3 cells/well) on a 96-well plate and cultured in DMEM/Ham's F-12 (1:1) medium supplemented with 5% FBS. After treatments (see figure legends), the cells were treated with 500 μg/ml of 3-(4,5-dimethysssl-thiazol-2-yl)2,5-diphenyl tetrazolium bromide (MTT; Sigma) and cultured for 3 h in a CO_2 incubator. The formazan crystals formed were solubilized in DMSO (Sigma) and measured with an ELx808 microplate spectrophotometer reader at $\lambda = 570$ nm (BioTek).

2.8. Cloning and DNA transfection

Rat IL-6 was generated by PCR using primers 5′-AAGAATTCATGAAGTTTCTCTCCGCAAG-3′ and 5′-AACTCGAGCTAGGTTTGCCGAGTAGA-3 from cDNA of Rat Kidney Quick Clone™ cDNA libraly (Clontech) as a template. The amplified fragment was digested with EcoRI and XhoI and inserted into pcDNA3-HA. HA-PGC-1α was kindly provided by Dr. Choi HS (Hormone Research Center, School of Biological Sciences and Technology, Chonnam National University, Korea). Podocytes were stabilized for 24 h before they were transfected with the pcDNA3-HA-IL6 and the pcDNA3-HA vector constructs. The culture medium was exchanged, and the constructs were transfected into the podocytes using Lipofectamine™ 2000 (Invitrogen), as instructed by the manufacturers.

2.9. siRNA transfection

Small interfering RNA (siRNA) motifs were synthesized according to the Ambion algorism rule by applying find pattern program to the rat IL-6 (GenBank number, NM_012589) and rat PGC-1α (GenBank number, NM_031347) cDNA sequences. The sequences of the 19-nucleotide (with two 5′ deoxy-thymidine overhangs) siRNA were as follows: IL-6, sense 5′-AACTTCCAATGCTCTCCTAATCCTGTCTC-3′, antisense 5′-AAATTAGGAGAGCATTGGAAGCCTGT- CTC-3 and PGC-1α, sense 5′ AAGACTATTGAGCGAACCTTACCTGTCTC-3′, antisense 5′-AATAAGGTTCGCTCAATAGTCCCTGTCTC-3. These siRNA primers were commercially synthesized (Bioneer, Daejeon,

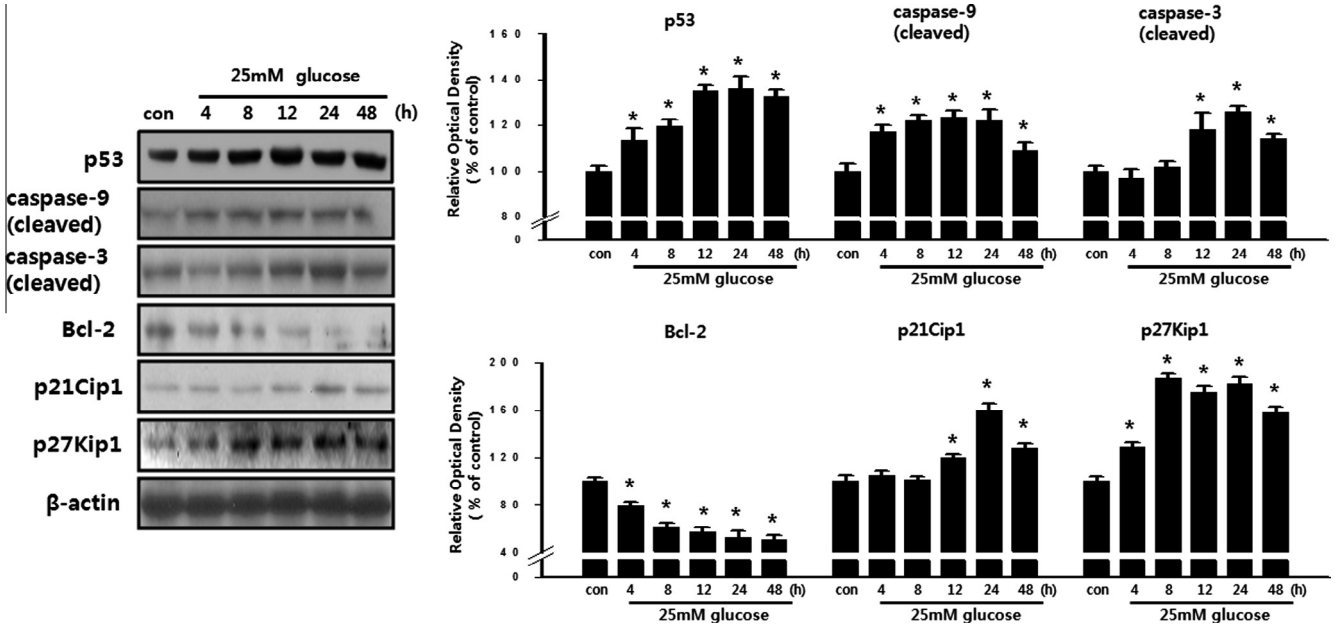

Fig. 1. The time dependency of high glucose on apoptotic molecules and growth arrest proteins in podocyte. Western blotting analysis of p53, caspase-9, caspase-3, Bcl-2, p21Cip, p27Kip and β-actin after the time dependent incubation of rat podocytes with 25 mM glucose. Target expression was normalized to that of β-actin and calculated relative to that of a control (see to 100%). Data represent the mean ± SE of three independent experiments, each performed in triplicate $^{*}p < 0.05$ *vs.* control.

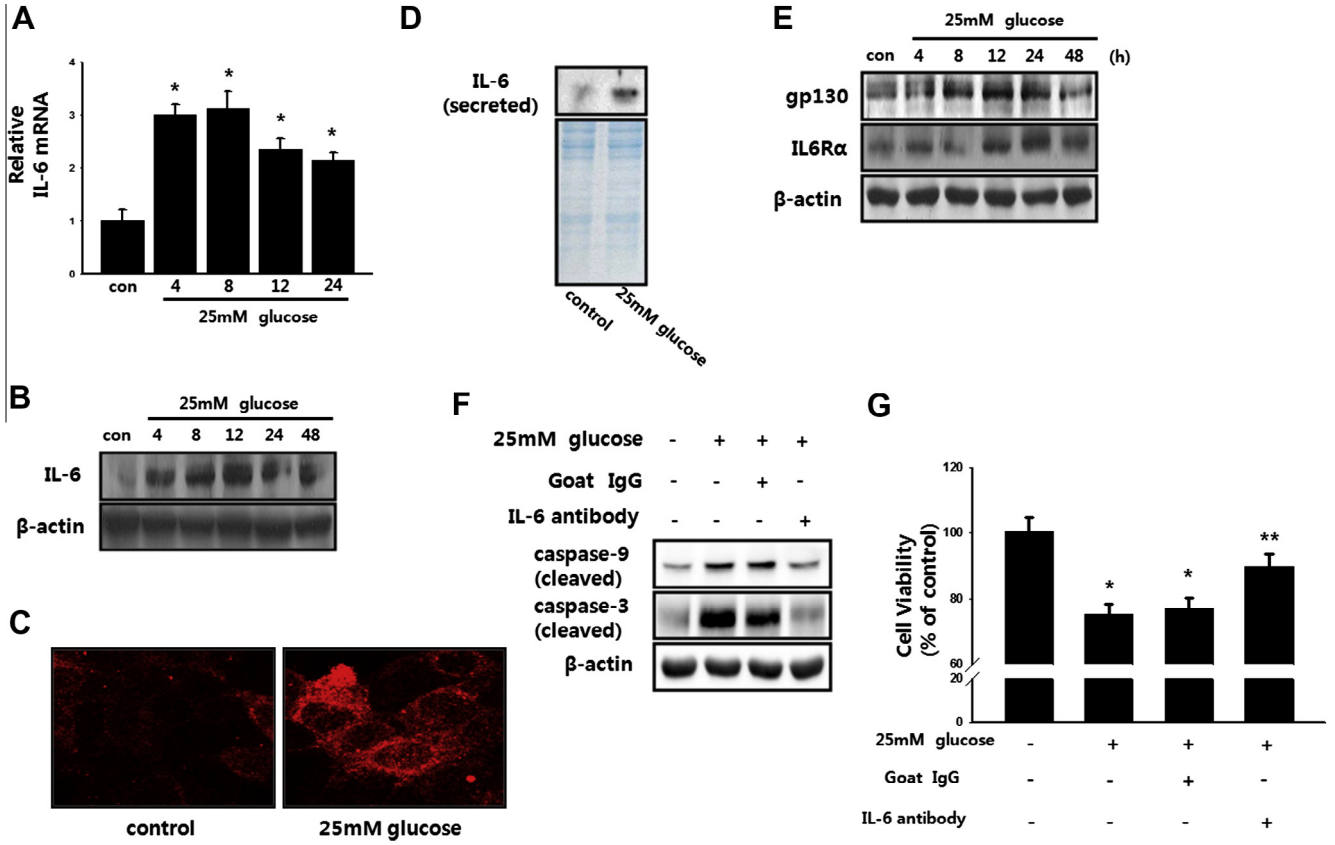

Fig. 2. The involvement of IL-6 on high glucose-induced podocyte apoptosis and growth arrest. (A) Real-time PCR analysis of IL-6 mRNA after the time dependent incubation of rat podocytes with 25 mM glucose. (B) Western blotting analysis of IL-6 and β-actin after the time dependent incubation of rat podocytes with 25 mM glucose. (C) Immunofluorescence analysis of IL-6 expression after 12 h incubation of rat podocytes with 25 mM glucose. (D) Western blotting analysis of secreted IL-6 by TCA precipitation of culture medium after 12 h incubation of rat podocytes with 25 mM glucose. (E) Western blotting analysis of gp130, IL6Rα and β-actin after the time dependent incubation of rat podocytes with 25 mM glucose. (F) Western blotting analysis of caspase-9, caspase-3 and β-actin after treatment of 25 mM glucose for 24 h with IL-6 neutralizing antibody or goat IgG. (G) Cell viability of rat podocytes measured by MTT assay after treatment of 25 mM glucose for 24 h with IL-6 neutralizing antibody or Goat IgG. Data represent the mean ± SE of three independent experiments, each performed in triplicate $^{*}p < 0.05$.

Korea) and synthesized and purified with Silence™ siRNA Construction Kit (Ambion, Austin, TX, USA). Transfection of IL-6, PGC-1α or scrambled siRNA was performed using Lipofectamine™ RNAiMAX Reagent (Invitrogen™, Carlsbad, CA, USA) according to the manufacturer's instructions. After 24 h, the podocytes were treated with 25 mM glucose.

2.10. Statistical analysis

The results were expressed as the mean ± the standard error (S.E.). Values are the mean ± S.E. of three or four independent experiments. All the experiments were analyzed by analysis of variance (ANOVA). In some experiments such as RT-PCR and western immunoblotting using inhibitors, a comparison of the treatment means was made with the control using the Bonferroni–Dunn test. A p value <0.05 was considered significant.

3. Results

3.1. The time-dependent effect of high glucose on podocyte apoptosis and podocyte growth arrest

To elucidate the effect of high glucose on podocytes, podocytes were exposed to 25 mM glucose for different time periods. As shown in Fig. 1, 25 mM glucose treatment significantly increased p53 protein expression and the cleaved forms of caspase-9 and caspase-3 in a time-dependent manner, peaking at 24 h, in the podocytes. Furthermore, 25 mM glucose treatment reduced Bcl-2 protein expression and increased p21Cip and p27Kip expression. These results suggest that high glucose induces not only podocyte apoptosis but also podocyte growth arrest.

3.2. The involvement of IL-6 in high glucose-induced podocyte apoptosis and growth arrest

To determine the effect of high glucose on IL-6 expression, podocytes were exposed to 25 mM glucose, and the mRNA was extracted for real-time PCR analysis. As shown in Fig. 2A, 25 mM glucose treatment increased IL-6 mRNA expression, which peaked at 8 h, and increased IL-6 protein expression (Fig. 2B). Increased IL-6 was detected predominantly around the cell membrane (Fig. 2C). Because IL-6 is a secreted protein, we extracted and analyzed the proteins from the medium used for podocyte culture. As shown in Fig. 2D, 25 mM glucose treatment stimulated podocyte secretion of IL-6 protein and increased the expression of gp130 and IL-6 receptor alpha (IL6Rα) (Fig. 2E). These data suggest that high glucose activates the IL-6 signaling cascade. Furthermore, studies with neutralizing antibody against IL-6 were performed to examine the involvement of IL-6 in high glucose-induced apoptosis. IL-6 antibody, but not IgG, abolished high glucose-induced stimulation of the cleaved forms of caspase-9 and caspase-3 (Fig. 2F). Additionally, IL-6 antibody, but not IgG, recovered the high glucose-induced decrease of cell viability (Fig. 2G). These results suggest that the increase in IL-6 secretion induced by high glucose mediates podocyte apoptosis.

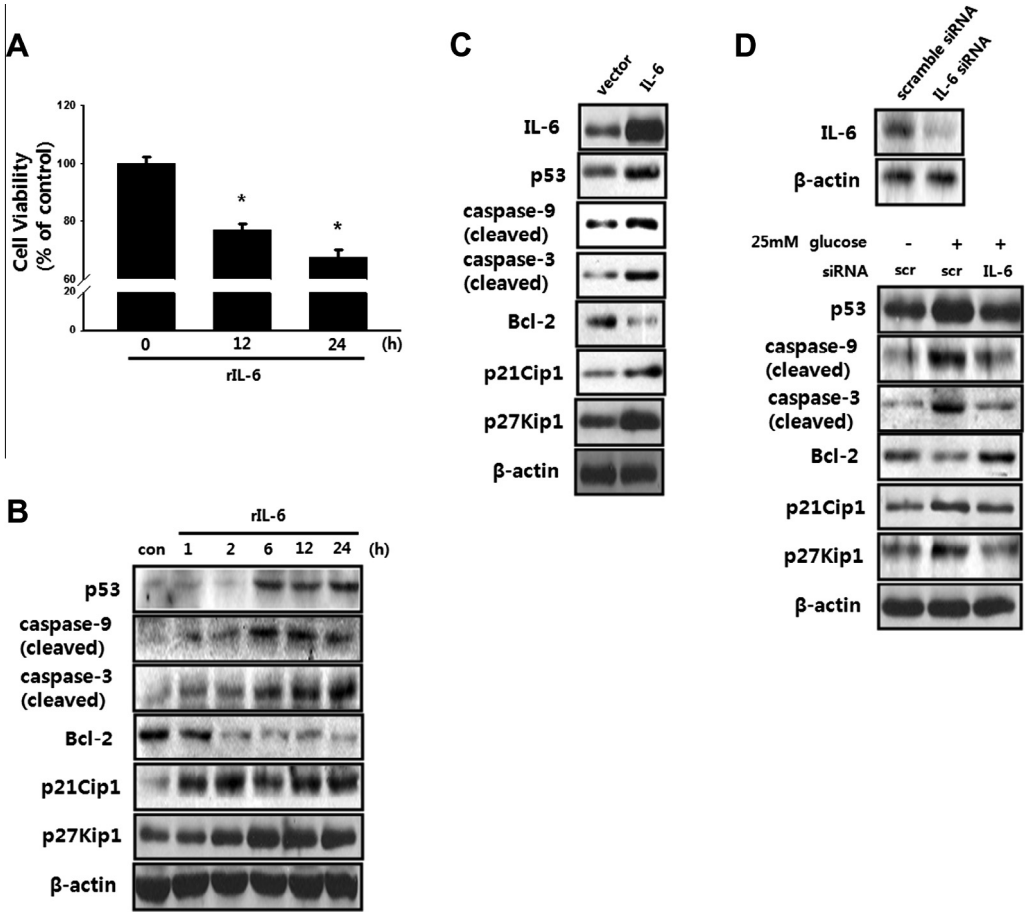

Fig. 3. The effect of IL-6 on podocyte apoptosis and growth arrest. (A) Cell viability of rat podocytes measured by MTT assay. (B) Western blotting analysis of indicated proteins after the time dependent incubation of rat podocytes with 1 nM IL-6. (C) Western blotting analysis of indicated proteins after 24 h incubation of HA (empty vector) or IL-6 transfected rat podocytes. (D) Western blotting analysis of indicated proteins after 24 h incubation of scramble or IL-6 siRNA transfected rat podocytes with 25 mM glucose $^{*}p < 0.05$.

3.3. The effect of IL-6 on podocyte apoptosis and growth arrest

To further examine the role of IL-6 in apoptosis, podocytes were treated with recombinant rat IL-6 (rIL-6). Fig. 3A shows that 1 nM rIL-6 decreased podocyte viability by up to 70% at 24 h and increased p53 protein expression and the cleaved forms of caspase-9 and caspase-3. In addition, rIL-6 decreased Bcl-2 protein expression and increased p21Cip and p27Kip expression (Fig. 3B). Assuming that secreted cellular IL-6 acts in a paracrine and/or autocrine manner in podocytes, an IL-6 plasmid was used for transient transfection. Overexpression of IL-6 induced an increase in p53 expression and the cleaved forms of caspase-9 and caspase-3. Additionally, IL-6 overexpression reduced Bcl-2 expression and increased p21Cip and p27Kip expression (Fig. 3C). To examine the loss of IL-6 function, IL-6 siRNA was used. Knockdown of IL-6 by siRNA diminished the high glucose-induced increase in p53 expression and the cleaved forms of caspase-9 and caspase-3. Moreover, knockdown of IL-6 recovered the high glucose-induced downregulation of Bcl-2 and upregulation of p21Cip and p27Kip expression (Fig. 3D).

3.4. The involvement of PGC-1α in high glucose-induced apoptosis and growth arrest

We also evaluated the involvement of PGC-1α in podocyte apoptosis and growth arrest. Glucose (25 mM) and rIL-6 each increased PGC-1α expression in a time-dependent manner (Fig. 4A, B). PGC-1α overexpression increased p53 expression and the cleaved forms of caspase-9 and caspase-3, reduced Bcl-2 expression and increased p21Cip and p27Kip expression (Fig. 4C). Knockdown of PGC-1α by siRNA diminished the high glucose-induced increase in p53 expression and the cleaved forms of caspase-9 and caspase-3. Additionally, knockdown of PGC-1α recovered the high glucose-induced downregulation of Bcl-2 and upregulation of p21Cip and p27Kip expression (Fig. 4D). Thus, PGC-1α may mediate high glucose-induced apoptosis and growth arrest.

4. Discussion

Recent studies have shown that high glucose stimulates the secretion of IL-6, which induces apoptosis *via* PGC-1α in a dose-dependent manner in podocytes. Souza et al. reported that serum IL-6 concentration is elevated in diabetic patients [12]. In particular, diabetic patients with nephropathy had a higher level of IL-6 than diabetic patients without nephropathy [13]. However, the pathophysiological role of IL-6 in podocytes in diabetic nephropathy is unclear. Based upon these reports, we hypothesized that IL-6 is involved in the development of diabetic nephropathy.

Our previous report revealed that high glucose induces podocyte loss, and the activation of CB1R and bradykinin receptor triggers apoptosis [14]. Several studies have reported similar results; high glucose increased caspase-3 and Bax, and decreased Bcl-2, suggesting a role in podocyte loss [15,16]. The present results showed that high glucose induces apoptosis by enhancing IL-6 secretion. First, high glucose and IL-6 induced apoptosis of rat podocytes. Second, high glucose increased the level of IL-6 mRNA expression and the levels of secreted IL-6 protein and IL-6 expression in podocytes. Third, anti-IL-6 antibody, but not IgG, blocked high glucose-induced apoptosis of podocytes. IL-6 binds to its specific receptor α-subunit, followed by the activation of the common receptor subunit, gp130 [6]. To date, the involvement of IL6Rα and gp130 in diabetes has not been examined simultaneously. Our present study provides new evidence that high glucose increases IL6Rα and gp130 expression in rat podocytes.

Tikoo et al. reported that p53 activation is implicated in the onset of diabetic nephropathy in type I diabetes models [17]. Our present results also demonstrated p53 pathway involvement in high glucose-induced apoptosis of rat podocytes; this is in agreement with Gao et al., who showed that high glucose-induced activation of the notch pathway *via* p53 activation is associated with podocyte loss [18]. Here, we presented additional evidence that IL-6 activation by high glucose is linked to the activation of p53, which eventually results in apoptosis of podocytes. Moreover,

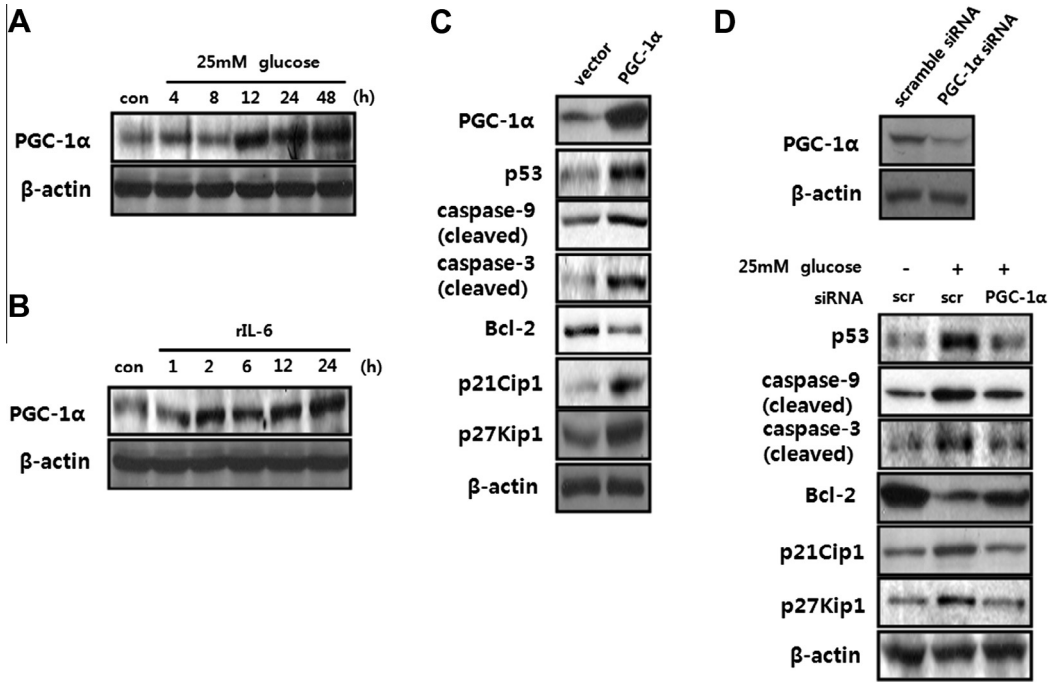

Fig. 4. The involvement of PGC 1-α on high glucose-induced apoptosis and growth arrest. (A) Western blotting analysis of PGC-1α and β-actin after the time dependent incubation of rat podocytes with 25 mM glucose. (B) Western blotting analysis of PGC-1α and β-actin after the time dependent incubation of rat podocytes with 1 nM IL-6. (C) Western blotting analysis of indicated proteins after 24 h incubation of HA (empty vector) or PGC-1α transfected rat podocytes. (D) Western blotting analysis of indicated proteins after 24 h incubation of scramble or PGC-1α siRNA transfected rat podocytes with 25 mM glucose.

our results implicate high glucose-induced activation of IL-6 secretion in cell cycle arrest and hypertrophy, as IL-6 siRNA blocked high glucose-induced stimulation of p21Cip1 and p27Kip1 expression. Several studies have indicated that high glucose-induced stimulation of p21Cip1 and p27Kip expression triggers hypertrophy in renal proximal tubule cells, suggesting a role in renal hypertrophy [19,20]. The result is evident *in vivo*: p21Cip and p27Kip expression in glomeruli was increased in kidneys of diabetic mice [21]. Baba et al. reported that high glucose upregulated p21Cip and p27Kip in mouse podocytes and that p27Kip1-positive cells in glomeruli are mainly podocytes in db/db mice [21]. Our results suggest that IL-6-associated alterations of p21Cip and p27Kip expression in podocytes may contribute to the onset of diabetic nephropathy. To our knowledge, this is the first report showing the stimulation of IL-6 secretion by high glucose-induced hypertrophy in podocytes.

Diverse signaling molecules are involved in podocyte loss, and PGC-1α is potentially important because it is expressed mainly in the kidney [22]. As the involvement of PGC-1α in the development of diabetic nephropathy is unclear, the present study examined the role of PGC-1α in high glucose-induced apoptosis. Our results revealed that PGC-1α was increased in response to high glucose, and PGC-1α siRNA (but not scrambled siRNA) prevented high glucose-induced apoptosis of rat podocytes. Furthermore, the overexpression of PGC-1α induced apoptosis of podocytes. These findings demonstrate that PGC-1α activation is closely linked to high glucose-induced apoptosis of podocytes. The present results are consistent with the report of Schilling & Kelly that PGC-1α activity is increased in the early stage of diabetes [23]. Koo et al. also found that PGC-1α promotes insulin resistance in the liver [24]. However, Gao et al. reported that high glucose decreased PGC-1α mRNA in 3T3-L1 adipocytes [25]. Several investigators have also reported that PGC-1α is responsible for the beneficial effect on energy metabolism of various cells [26,27]. This discrepancy among studies may be attributable to the use of different species (rat *vs*. mouse) or cell types (podocyte *vs*. adipocyte). We speculated that PGC-1α may have contradictory effects in various cell types and that PGC-1α has a negative effect in podocyte function. Podocyte-specific PGC-1α knockout mice should be engineered to confirm the exact function of PGC-1α in diabetic nephropathy. In this study, we provide evidence that PGC-1α is an important downstream mediator of IL-6 activation induced by high glucose, which is involved in cell growth arrest and apoptosis of podocytes.

Collectively, these results identified a novel connection between high glucose and IL-6 activation, which promoted apoptosis and cell growth arrest in podocytes *via* IL6Rα and gp130. In addition to its beneficial role in many cells, PGC-1α expression appears to be involved in apoptosis under pathophysiological conditions. Therefore, blocking IL-6 and its downstream mediators such as IL6Rα, gp130 and PGC-1α may attenuate the progression of diabetic nephropathy. Identifying this pathway will help to elucidate the molecular events leading to the activation of IL-6-mediated apoptosis in diabetic nephropathy and may contribute to the design of new therapeutic strategies for diabetic nephropathy.

Acknowledgment

This study was supported financially by a research Grant from the Korean Science & Engineering Foundation (2010-0023627).

References

[1] S.C. Satchell, The glomerular endothelium emerges as a key player in diabetic nephropathy, Kidney Int. 82 (2012) 949–951.
[2] M. Miyauchi, M. Toyoda, K. Kobayashi, M. Abe, T. Kobayashi, M. Kato, N. Yamamoto, M. Kimura, T. Umezono, D. Suzuki, Hypertrophy and loss of podocytes in diabetic nephropathy, Intern. Med. 48 (2009) 1615–1620.
[3] S. Menini, C. Iacobini, G. Oddi, C. Ricci, P. Simonelli, S. Fallucca, M. Grattarola, F. Pugliese, C. Pesce, G. Pugliese, Increased glomerular cell (podocyte) apoptosis in rats with streptozotocin-induced diabetes mellitus: role in the development of diabetic glomerular disease, Diabetologia 50 (2007) 2591–2599.
[4] C.J. Kuan, M. al-Douahji, S.J. Shankland, The cyclin kinase inhibitor p21WAF1, CIP1 is increased in experimental diabetic nephropathy: potential role in glomerular hypertrophy, J. Am. Soc. Nephrol. 9 (1998) 986–993.
[5] S. Muller-Krebs, L.P. Kihm, T. Madhusudhan, B. Isermann, J. Reiser, M. Zeier, V. Schwenger, Human RAGE antibody protects against AGE-mediated podocyte dysfunction, Nephrol. Dial. Transpl. 27 (2012) 3129–3136.
[6] Y. Fujio, M. Maeda, T. Mohri, M. Obana, T. Iwakura, A. Hayama, T. Yamashita, H. Nakayama, J. Azuma, Glycoprotein 130 cytokine signal as a therapeutic target against cardiovascular diseases, J. Pharmacol. Sci. 117 (2011) 213–222.
[7] H. Esterbauer, H. Oberkofler, F. Krempler, W. Patsch, Human peroxisome proliferator activated receptor gamma coactivator 1 (PPARGC1) gene: cDNA sequence, genomic organization, chromosomal localization and tissue expression, Genomics 62 (1999) 98–102.
[8] C. Canto, J. Auwerx, PGC-1α, SIRT1 and AMPK, an energy sensing network that controls energy expenditure, Curr. Opin. Lipidol. 20 (2009) 98–105.
[9] J. Shoag, Z. Arany, Regulation of hypoxia-inducible genes by PGC-1 α, Arterioscler., Thromb., Vasc. Biol. 30 (2010) 662–666.
[10] C.R. Benton, G.P. Holloway, X.X. Han, Y. Yoshida, L.A. Snook, J. Lally, J.F. Glatz, J.J. Luiken, A. Chabowski, A. Bonen, Increased levels of peroxisome proliferator-activated receptor gamma, coactivator 1 α (PGC-1α) improve lipid utilisation, insulin signalling and glucose transport in skeletal muscle of lean and insulin-resistant obese Zucker rats, Diabetologia 53 (2010) 2008–2019.
[11] J.I. Kreisberg, R.L. Hoover, M.J. Karnovsky, Isolation and characterization of rat glomerular epithelial cells *in vitro*, Kidney Int. 14 (1978) 21–30.
[12] J.R. Souza, R.T. Oliveira, M.H. Blotta, O.R. Coelho, Serum levels of interleukin-6 (Il-6), interleukin-18 (Il-18) and C-reactive protein (CRP) in patients with type-2 diabetes and acute coronary syndrome without ST-segment elevation, Arq. Bras. Cardiol. 90 (2008) 86–90.
[13] A. Taslipinar, H. Yaman, M.I. Yilmaz, S. Demirbas, M. Saglam, M.Y. Taslipinar, M. Agilli, Y.G. Kurt, A. Sonmez, O. Azal, E. Bolu, M. Yenicesu, M. Kutlu, The relationship between inflammation, endothelial dysfunction and proteinuria in patients with diabetic nephropathy, Scand. J. Clin. Lab. Inv. 71 (2011) 606–612.
[14] S.K. Lim, S.H. Park, The high glucose-induced stimulation of B1R and B2R expression *via* CB(1)R activation is involved in rat podocyte apoptosis, Life Sci. 91 (2012) 895–906.
[15] G.M. Mitu, S. Wang, R. Hirschberg, BMP7 is a podocyte survival factor and rescues podocytes from diabetic injury, Am. J. Physiol. Ren. Physiol. 293 (2007) F1641–F1648.
[16] E.B. Peixoto, A. Papadimitriou, J.M. Lopes de Faria, J.B. Lopes de Faria, Tempol reduces podocyte apoptosis *via* PARP signaling pathway in experimental diabetes mellitus, Nephron Exp. Nephrol. 120 (2012) e81–e90.
[17] K. Tikoo, K. Singh, D. Kabra, V. Sharma, A. Gaikwad, Change in histone H3 phosphorylation, MAP kinase p38, SIR 2 and p53 expression by resveratrol in preventing streptozotocin induced type I diabetic nephropathy, Free Radic. Res. 42 (2008) 397–404.
[18] F. Gao, M. Yao, Y. Shi, J. Hao, Y. Ren, Q. Liu, X. Wang, H. Duan, Notch pathway is involved in high glucose-induced apoptosis in podocytes *via* Bcl-2 and p53 pathways, J. Cell. Biochem. 114 (2013) 1029–1038.
[19] L. Sun, V.K. Kondeti, P. Xie, K. Raparia, Y.S. Kanwar, Epac1-mediated, high glucose-induced renal proximal tubular cells hypertrophy *via* the Akt/p21 pathway, Am. J. Pathol. 179 (2011) 1706–1718.
[20] J.S. Huang, L.Y. Chuang, J.Y. Guh, Y.J. Huang, M.S. Hsu, Antioxidants attenuate high glucose-induced hypertrophic growth in renal tubular epithelial cells, Am. J. Physiol. Ren. Physiol. 293 (2007) F1072–F1082.
[21] M. Baba, J. Wada, J. Eguchi, I. Hashimoto, T. Okada, A. Yasuhara, K. Shikata, Y.S. Kanwar, H. Makino, Galectin-9 inhibits glomerular hypertrophy in db/db diabetic mice *via* cell-cycle-dependent mechanisms, J. Am. Soc. Nephrol. 16 (2005) 3222–3234.
[22] S.N. Schreiber, D. Knutti, K. Brogli, T. Uhlmann, A. Kralli, The transcriptional coactivator PGC-1 regulates the expression and activity of the orphan nuclear receptor estrogen-related receptor α (ERRalpha), J. Biol. Chem. 278 (2003) 9013–9018.
[23] J. Schilling, D.P. Kelly, The PGC-1 cascade as a therapeutic target for heart failure, J. Mol. Cell. Cardiol. 51 (2011) 578–583.
[24] S.H. Koo, H. Satoh, S. Herzig, C.H. Lee, S. Hedrick, R. Kulkarni, R.M. Evans, J. Olefsky, M. Montminy, PGC-1 promotes insulin resistance in liver through PPAR-alpha-dependent induction of TRB-3, Nat. Med. 10 (2004) 530–534.
[25] C.L. Gao, C. Zhu, Y.P. Zhao, X.H. Chen, C.B. Ji, C.M. Zhang, J.G. Zhu, Z.K. Xia, M.L. Tong, X.R. Guo, Mitochondrial dysfunction is induced by high levels of glucose and free fatty acids in 3T3-L1 adipocytes, Mol. Cell. Endocrinol. 320 (2010) 25–33.
[26] P. Wareski, A. Vaarmann, V. Choubey, D. Safiulina, J. Liiv, M. Kuum, A. Kaasik, PGC-1α and PGC-1β regulate mitochondrial density in neurons, J. Biol. Chem. 284 (2009) 21379–21385.
[27] D. Mirebeau-Prunier, S. Le Pennec, C. Jacques, N. Gueguen, J. Poirier, Y. Malthiery, F. Savagner, Estrogen-related receptor α and PGC-1-related coactivator constitute a novel complex mediating the biogenesis of functional mitochondria, FEBS J. 277 (2010) 713–725.